Available online at www.sciencedirect.com
ScienceDirect
Catalysis Today 128 (2007) 258–263
CATALYSIS TODAY
www.elsevier.com/locate/cattod

Effect of silicates on the structure of Ni-containing catalysts obtained from hydrotalcite-type precursors

S. Albertazzi [a], F. Basile [a], P. Benito [a,*], P. Del Gallo [b], G. Fornasari [a], D. Gary [b], V. Rosetti [a], A. Vaccari [a]

[a] *Dip. Chim. Ind. e dei Mat., Univ. di Bologna, V.le Risorgimento 4, 40136 BO, Italy*
[b] *Air Liquide, Centre de Recherche Claude Delorme 1, Chemin de la Porte des Loges, BP 126, Les Loges-en-Josas, 78354 Jouy-en-Josas Cedex, France*

Available online 20 August 2007

Abstract

New nickel hydrotalcite-like compounds with silicates as interlayer anions used as catalyst precursors in the catalytic partial oxidation of methane were prepared by the coprecipitation method. The properties of these materials were compared with those of compounds obtained from carbonate-containing materials. The precursors and calcined samples were characterized by powder X-ray diffraction, FT-IR and Vis/UV/NIR spectroscopies, thermal analyses (DTA and TG), temperature programmed reduction (TPR) and N_2 adsorption/desorption at −196 °C. The results show that the incorporation of silicates in the lamellar compounds modifies the structural and textural properties of the precursors. After calcination, silicates – which are non-volatile anions – contribute to the final structure of the catalysts, which form a new forsterite-like phase, increasing their specific surface area but not altering the reducibility of the nickel species.

Keywords: Hydrotalcite; Silicate; Catalyst; Mixed oxide; Forsterite

1. Introduction

Hydrotalcite-like compounds are lamellar materials with the chemical formula $[M^{2+}_{1-x}M^{3+}_{x}(OH)_2]\ (A^{n-})_{x/n}\cdot nH_2O$. A wide variety of compounds have been synthesized by modifying both the lamellar and the interlamellar region; materials especially designed to meet specific requirements have been prepared. HTlcs have been largely used as precursors of catalysts and supports in organic processes, as environmental catalysts, hydrogenation catalysts, and in natural gas conversion [1–8].

The high affinity of hydrotalcite-like materials to carbonate species has mostly led to the use of carbonate-containing compounds as precursors of catalysts. After calcination at approximately 250 °C, the interlamellar water is released; by increasing the temperature to 450–550 °C, lamellar collapse occurs, with the elimination of hydroxyl groups as water molecules and carbonate anions as carbon dioxide. The products obtained at this stage are oxides forming a solid solution, i.e. mixed oxides. Temperature increases lead to the segregation of phases, spinel and pristine oxides. Compared to impregnated catalysts, calcination products obtained by the decomposition of HTlcs offer advantages such as a relatively large specific surface area, high thermal stability, and – most importantly – high and stable interdispersion of the active species with high reproducibility. The latter is a consequence of the original structure of the lamellar compound, where the atoms occupy random positions throughout the layers, and the decomposition takes place topotactically; thus the cations maintain their original location in the calcined products and, after reduction, metallic species highly dispersed in an inert matrix are obtained.

However, another advantage when using HTlcs as precursors is that their composition can be easily modified by replacing not only the lamellar structure but, as previously seen, also the species located in the interlayer. In fact, the LDH anion-exchange capacity has been used in catalysis as a tool to introduce components offering a target activity and/or selectivity. In addition, the intercalation of some anions may introduce cations which are not compatible with the octahedral sites of the brucite-type sheets.

* Corresponding author. Tel.: +39 0512093677; fax: +39 0512093679.
E-mail address: pbenito@ms.fci.unibo.it (P. Benito).

0920-5861/$ – see front matter © 2007 Elsevier B.V. All rights reserved.
doi:10.1016/j.cattod.2007.06.067

This is the case of HTlcs-containing silicate, used as precursor of catalysts, which have shown improved catalytic performance in the catalytic partial oxidation of methane (CPO) [9] even at low nickel load [10]. The derived catalysts present higher CH_4 conversion and CO and H_2 selectivity than those with the same formulation but obtained from a HT-containing carbonates, in which the spinel-type phase was present [9]. Unlike carbonate anions, they do not decompose into volatile species when calcined at high temperatures, thus contributing to the stability and performance of the final catalysts. Different synthetic routes have been described to prepare HTlcs-containing silicates, such as ion exchange by using different silicate precursors – SiO_2 in NaOH [11–13], octasilicate ion [14], TEOS [15], and/or sodium metasilicate [16,17] and precipitation using Na_2SiO_3 as silicate source [17].

In the present study, a $Ni_8Mg_{60}Al_{32}$ HTlc with silicates as counterbalance anions was synthesized by the simple coprecipitation method. A 20% excess of silicates was used, compared to the amount required to balance the charge excess, since when they are intercalated some polymeric species are formed. The theoretical chemical formula is $[Ni_{0.080}Mg_{0.600}Al_{0.320}(OH)_2](Si_nO_{2n+1}{}^{2-})_{0.192}\cdot nH_2O$. The lamellar compound was calcined at 900 °C to obtain the catalyst which is active in the CPO process with a Ni 8.08 wt.%. Physicochemical and textural properties of the materials were studied in order to clarify their improved catalytic performance. For comparison purposes, a carbonate-containing compound with the same nickel load when calcined (8.058%) and M^{2+}/M^{3+} ratio was also synthesized $[Ni_{0.063}Mg_{0.617}Al_{0.320}(OH)_2]\ (CO_3{}^{2-})_{0.160}\cdot nH_2O$.

2. Experimental

2.1. Synthesis

The silicate-containing sample was prepared following the coprecipitation method at constant pH. A 0.2 M solution containing the nitrate salts of anions in the appropriate ratios was slowly added to a solution containing silicates (sodium silicate solution, NaOH (≥10%), SiO_2 (≥27%), Aldrich). pH was kept constant by NaOH addition (10.5 ± 0.2). The addition of the cation solution took place for 20 min; the obtained precipitate was kept in suspension by stirring at 60 °C for 45 min, then filtered and washed with distilled water until a Na_2O content lower than 0.02 wt.% was obtained. The precipitate was dried overnight at 60 °C. The hydrotalcite-type precursor with carbonate was synthesized following the same coprecipitation method. Catalysts were obtained by calcination, heated at a rate of 10 °C min^{-1} from room temperature up to 900 °C and kept at 900 °C for 12 h. The samples were named as follows: HT carbonate and HT silicate for the precursors and exHT carbonate and exHT silicate for the calcined solids.

2.2. Characterization

XRD powder analyses were carried out using a Philips PW1050/81 diffractometer equipped with a graphite monochromator in the diffracted beam and controlled by a PW1710 unit (λ = 0.15418 nm). A 2θ range from 10° to 80° was investigated at a scanning speed of 70°/h. The FT-IR spectra were recorded by the Attenuated Reflectance Technique on a Perkin-Elmer Spectrum One FT-IR Spectrometer with a Universal ATR Sampling Accessory. UV-Vis/NIR spectra were recorded using the diffuse reflectance (UV-Vis-NIR/DR) technique in a Perkin-Elmer Lambda 19 and software UV WinLab, using 2 nm slits and MgO as a reference. Thermogravimetric (TG) and differential thermal analyses (DTA) were carried out in TGA 2050 and 1600 DTA instruments from TA instruments, respectively, in flowing air, at a heating rate of 10 °C min^{-1}. The TPR analyses were carried out with an H_2/Ar 5/95 (v/v) (total flow rate 20 ml/min) gas mixture in the 100–950 °C temperature range in a ThermoQuest CE TPDRO 1100 instrument. Specific surface area assessment was carried out in a Micromeritics ASAP 2020 instrument. The precursors were previously degassed under a vacuum at 120 °C until a pressure of 30 μmHg was reached and maintained for 30 min. Calcined solids were heated up to 150 °C until a pressure of 30 μmHg was reached, then kept 30 min at this temperature and finally heated up to 250 °C and maintained for 30 min.

3. Results and discussion

3.1. Hydrotalcite-like compounds

PXRD patterns of the carbonate- and silicate-containing compounds are shown in Fig. 1. The pattern of the HT carbonate sample shows the characteristic diffraction pattern of hydrotalcite-like compounds with sharp and intense diffraction lines due to basal reflection lines and broad and less intense peaks related with non-basal planes; the basal spacing is 7.6 Å [1]. The insertion of silicates, rather than carbonates, in the interlayer leads to a solid with a lower crystalline degree and with a rather similar basal spacing (only a slight shift towards lower 2θ values is observed). Decreased crystallinity is observed not only in the basal direction but also within layers, as can be seen by the considerable reduction in the intensity of the first reflection line and the poor resolution of the doublet

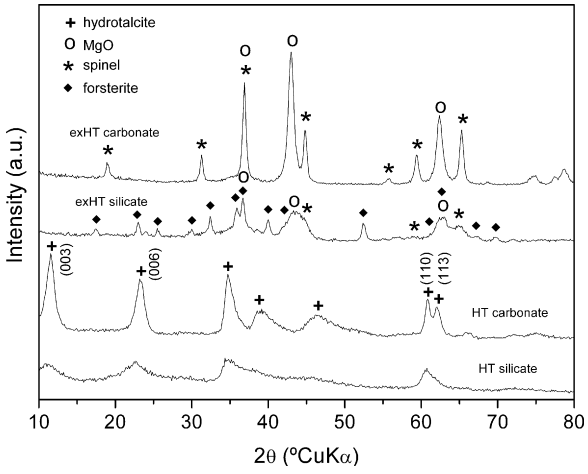

Fig. 1. PXRD patterns of the HT carbonate and HT silicate samples, precursors and catalysts.

(recorded in the 60–65° 2θ range) due to the ((1 1 0) and (1 1 3)) diffraction planes.

The basal spacing obtained in the compound synthesized here is lower than the 12 Å reported by other authors [11], but it is similar to the value obtained by Dèpege et al. [17]. This low basal spacing was explained by Dèpege et al. as due to the formation of polysilicate where SiO_4 units condense with the same orientation. Moreover a grafting process of silicate layers onto brucite-like layers with a diffusion of Al^{3+} ions from the layers occurred during preparation [17]. However, in the solids prepared, the presence of some silicate species adsorbed on the particle surface cannot be ruled out.

FT-IR spectroscopy can also give useful information about the structure of the compounds and interlamellar anions. The FT-IR spectra of the LDH precursors are shown in Fig. 2. They show the characteristic bands of hydrotalcite-like compounds [18]. The broad band at 3400 cm^{-1} is attributed to the $\nu_{(OH)}$ vibration mode of lamellar OH groups and water molecules, either inserted in the interlamellar space or physisorbed on the surface. Furthermore, at around 1640 cm^{-1} the bending mode of water molecules is also observed. It should be noted that, in the spectrum of the carbonate-containing sample, the shoulder at around 2900 cm^{-1} is recorded, whereas the shoulder cannot be observed in silicate spectra. This shoulder is attributed to OH groups bonded to carbonate species in the interlayer region [19], therefore it should not be recorded in the silicate-containing sample. However, at around 1365 cm^{-1} the band due to the $\nu_3(CO_3^{2-})$ vibration mode is recorded for both samples, thus suggesting contamination by carbonate species, because of the high affinity of these species to HTlcs. In addition, the infrared spectrum of the HT silicate sample shows a strong Si–O stretching band at around 995 cm^{-1} characteristic of silicate moieties, due to the antisymmetric ν_3(Si–O) vibration mode. Neither band is recorded at 800 cm^{-1} (ν_1(Si–O)) or 1200 cm^{-1} (δ(Si–O–Si)). The absence of the latter band suggests the condensation of SiO_4 octahedron with the same orientation in the interlayer. This feature agrees with the data obtained by PXRD, since the basal spacing obtained is lower than that expected in an inverted connecting frame between two straight-linked SiO_4 tetrahedral groups. On the other hand, the absence of ν_1(Si–O) mode indicates that no reduction in the symmetry of the silicon atom occurs in the polysilicate. Lastly, the lower wavenumber region provides information about the intralamellar order. In this region, lattice vibration modes are recorded. These bands are not resolved in the HT-silicate sample: a feature that agrees with the low order within layers, which is supported by the poor resolution of the (1 1 0) and (1 1 3) diffraction lines.

TG and DTG curves for the HT-silicate sample are shown in Fig. 3. Two weight losses are observed. The first corresponds to the removal of physisorbed and interlamellar water, and the second to the dehydroxilation and removal of the contaminant carbonate species present in the compound [20]. The DTG curve provides more detailed information about the decomposition process. It is possible to distinguish perfectly two overlapping peaks in the region below 200 °C, corresponding to the removal first of physisorbed and then of interlayer water; the high intensity of the former peak could be related to the low crystallinity of the compound. It should be noted that the final weight is around 62% of the initial weight: a value greater than the 55% obtained in the case of the carbonate sample, since

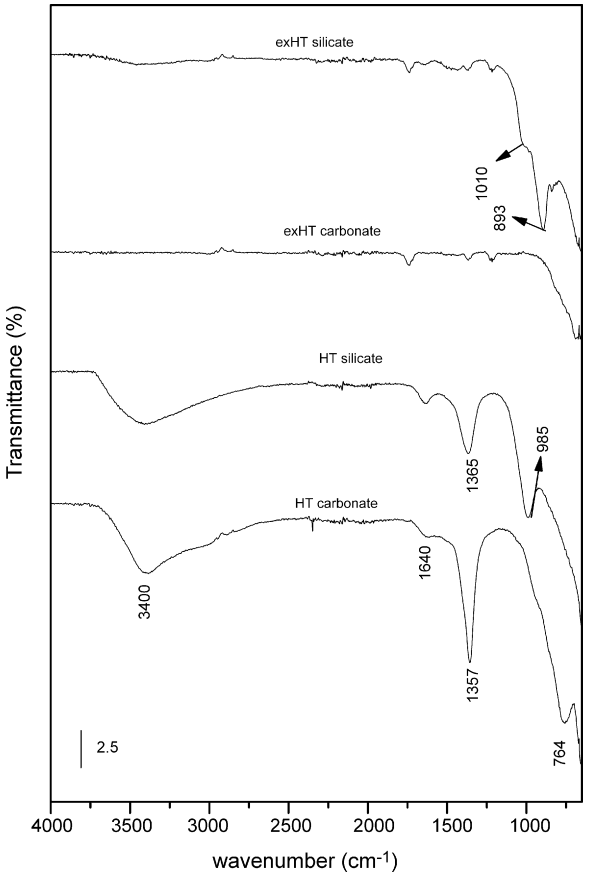

Fig. 2. FT-IR spectra of the HTlcs and calcined solids.

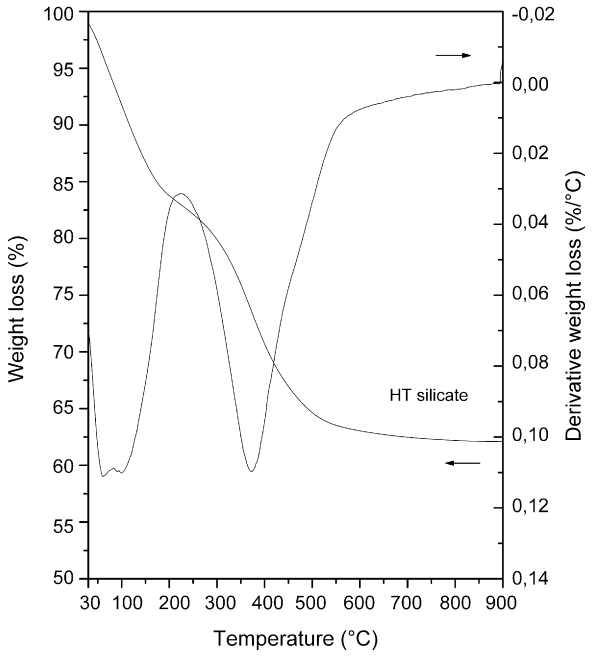

Fig. 3. TG and DTG curves of the HTlc-containing silicate samples.

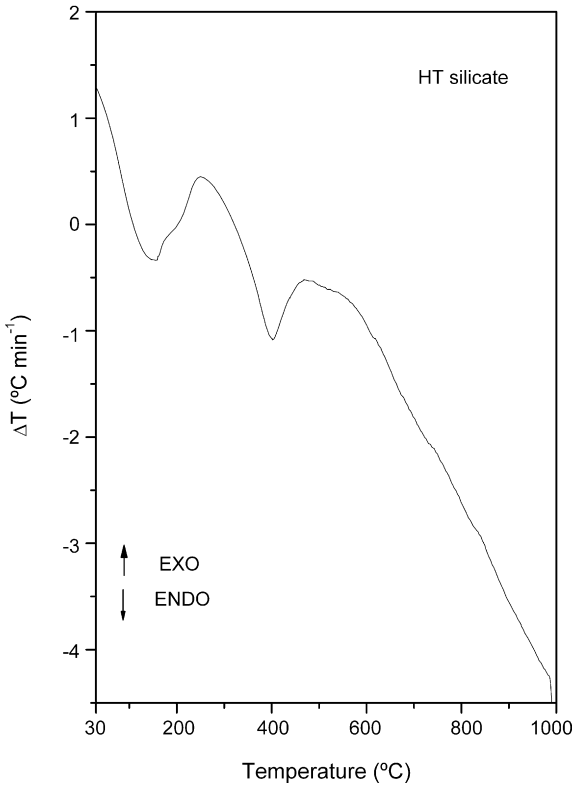

Fig. 4. DTA of the HTlc-containing silicate sample.

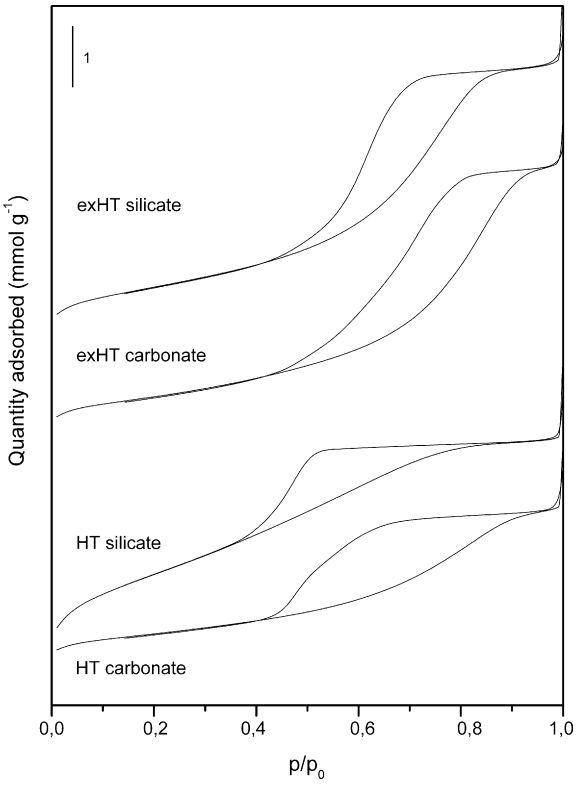

Fig. 5. N_2 Adsorption/desorption isotherms of the HTlcs and the calcined solids.

non-volatile silicate anions remain in the structure of the catalysts after calcination. Weight losses occur at temperatures similar to those of carbonate-containing compounds; thus the thermal stability is mainly determined by the nature of the hydroxide layers rather than interlamellar anions [14]. The DTA curve of the HT-silicate sample shows two endothermic peaks corresponding to the above-mentioned weight losses (Fig. 4). However, no exothermic peak at around 850 °C is observed, as was previously reported by other authors, because of the formation of the forsterite structure [14].

Values of specific surface areas were calculated following the B.E.T. method. The incorporation of silicates into the structure leads to a significant development of the specific surface area: it increases from 52 $m^2\,g^{-1}$ for the carbonate sample to 200 $m^2\,g^{-1}$ for the silicate compound. Reported isotherms (Fig. 5) belong to the Type IV in the IUPAC classification corresponding to adsorption on mesoporous solids, i.e. at high pressure, beyond a given point, there is no more uptake of gas despite the further pressure increase [21]. Curves present a very broad Type H2 hysteresis, with a long and almost flat ‘‘plateau’’ and a steep desorption branch. This hysteresis loop is characteristic of solids whose pore structures are complex and tend to be made up of interconnected networks of pores of different sizes and shapes (in which both pore size distribution and pore shape are not well defined) [22]. The fact that the plateau is reached at different relative pressures for HT-silicate is an indication that the mesopore structure is modified by the incorporation of silicates. The Barret–Joyner–Hallenda (BJH) desorption curve (Fig. 6) for the silicate-containing sample shows a narrow monomodal distribution of pore size

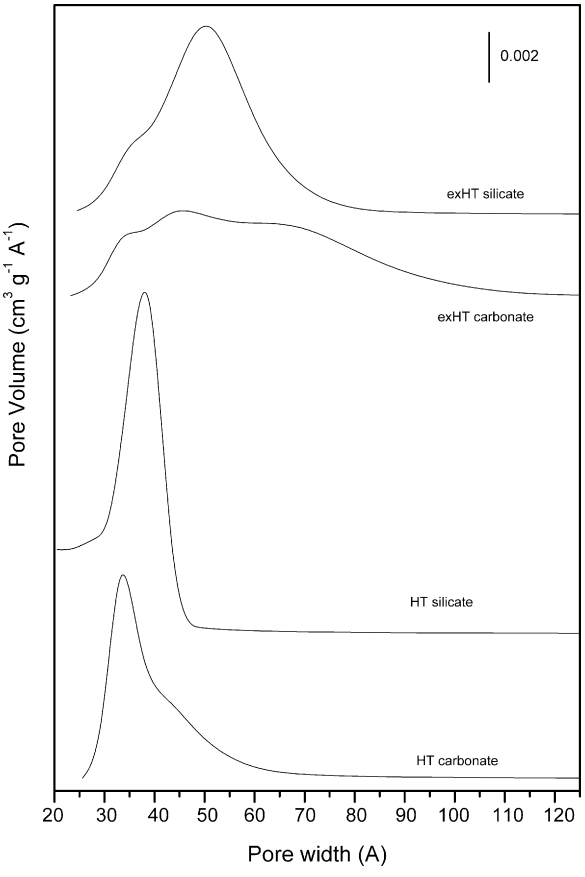

Fig. 6. BJH pore size distribution of the precursors and the catalysts.

with a peak at 39 Å, whereas for the carbonate compound, larger pores are also developed together with the pores of around 33 Å, since they are responsible for the adsorption at higher p/p_0 values. It should be taken into account that hydrotalcite-like compounds are non-porous or macroporous materials, so the mesopores detected here should be formed by the aggregation of hexagonal particles, which is also related to their size. Therefore, it could be concluded that the interlamellar anion greatly determines the textural properties of the HTlcs by modifying the size or aggregation of the individual particles.

3.2. Calcined products

After calcination at 900 °C, a spinel-type phase and a rock-salt phase are obtained for the HT carbonate sample (Fig. 1). In this catalyst, nickel cations are well dispersed into the MgO phase, forming a solid solution [23]. On the other hand, by calcining the HT silicate sample a more complex pattern is obtained. New diffraction peaks assigned to a forsterite-like phase (Mg_2SiO_4) are indexed; conversely, no well-defined phase containing Al ($MgAl_2O_4$) was detected, while the MgO phase is still present. The forsterite phase is a nesosilicate, orthosilicate phase (olivine class) characterized by isolated SiO_4^{4-} connected with Mg in octahedral coordination with oxygen. The stability of this phase is provided by the isolation of the SiO_4^{4-} group that are bonded to other cations, thus originating a stable thermodynamic phase and a strong inhibiting effect on its decomposition and vaporization [24]. Some reflection lines due to a spinel-type phase are observed in the diffraction patterns; however, they are weak and broad and the first two reflections at 19 and 32° 2θ ascribed to (1 1 1) and (2 2 0) are not observed, thus suggesting the formation of a defective spinel phase. It would appear that the presence of silicates which react with MgO to form the forsterite phase affects and possibly delays the formation of the spinel phase. In this catalyst, nickel cations might not only be located in the MgO phase forming the ($Mg_{(x)}Ni_{(1-x)}O$) solid solution, but might also be incorporated into the forsterite-like structure in the octahedral holes, as was previously reported for Ni-doped forsterite compounds [25], and form a $NiAl_2O_4$ phase. The poor resolution of the diffraction patterns makes it impossible to calculate cell parameters in the forsterite phase, which would help elucidate the incorporation of aluminum and nickel species in the silicate structure.

The Vis/UV/NIR spectra (not shown) are similar regardless of the catalyst. They show characteristic bands due to the transitions of Ni^{2+} ions located in an octahedral environment [26]. No clear bands ascribed to tetrahedral Ni^{2+} ions are observed in the spectra; however, for silicate catalysts, the $NiAl_2O_4$ formation cannot be completely discarded due to the complex catalyst structure. It should be noted only that there is a shift towards lower wavelengths for the calcined solids in comparison to the lamellar compounds.

Temperature programmed reduction (TPR) completed the study, to check the reducibility of the catalysts. TPR profiles show a single H_2 consumption peak at around 950 °C (see Fig. 7). High reduction temperatures are a consequence of the formation of the solid solution in which high metal-support interactions are established; these interactions delay the reduction of the active species [23].

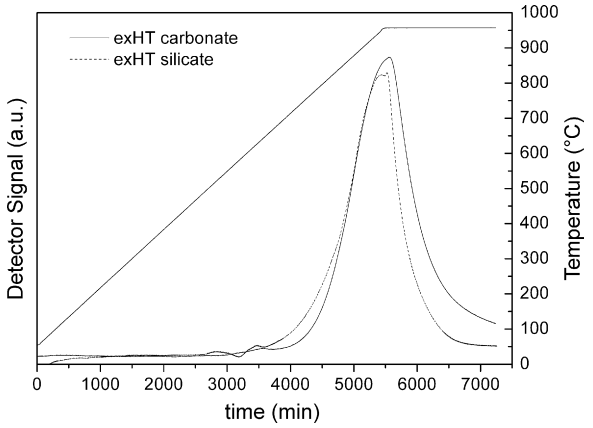

Fig. 7. Temperature programmed reduction profiles of the catalysts.

In order to complete the structural characterization of catalysts, FT-IR spectra were registered (Fig. 2). No information can be obtained from the spectrum of the exHT carbonate sample since the vibration modes owing to the oxide and spinel phases are outside of the spectral range of the instrument. However, some information can be obtained about silicate groups for the exHT silicate sample. The intense band due to the Si–O stretching is still recorded, although some changes are observed. The minimum is shifted toward lower energies, 895 cm^{-1}, and a shoulder is recorded at around 1000 cm^{-1}. The change in the stretching band might be due to a modification in the environment of SiO_4 units; in fact, in non-calcined solids, silicon atoms form Si–O–Si bonds, whereas in the forsterite-like compound Si–O–Mg links are formed. In addition, the partial replacement of magnesium cations with aluminum or nickel cations cannot be discarded.

Finally, the textural properties of the catalyst were studied. Calcination at high temperatures yields a decrease in the S_{BET} area for the exHT silicate sample (96 $m^2\ g^{-1}$), whereas an increase in the area is observed for the exHT carbonate catalyst (68 $m^2\ g^{-1}$). It is widely accepted that the decomposition process of HTlcs intercalated with carbonate occurs through the removal of CO_2 and H_2O by a ''cratering'' mechanism [27]. This behavior is responsible for the increase in the S_{BET} area for solids calcined at moderate temperatures (400–600 °C); a segregation of MgO and $MgAl_2O_4$ type phases, leading to both the sinterization process and a reduction in the specific surface area, then takes place. The increased S_{BET} area for carbonate samples may be related to the increased area at moderate temperatures, which is not greatly reduced by increasing the calcination temperature, because these compounds are stable against sinterization. On the other hand, for silicate samples, first of all, since the anions located in the interlayer are mainly polysilicates (although the presence of some carbonates cannot be ruled out), the ''cratering'' mechanism would lead to a lesser increase of the S_{BET}. On the other hand, the phase segregation pathway is different for silicate catalysts: in this case, together with the MgO and spinel phases, a well crystallized forsterite

phase is formed, which may be responsible for the decreased S_{BET}. Furthermore, isotherms change after the thermal treatment; more specifically, the hysteresis loop is altered (Fig. 5). Hysteresis curves belong to the Type H1, the loop is narrower, and the desorption branches are nearly parallel. Rouquerol et al. named these kinds of isotherms Type IVa [22]. In addition, the Barret–Joyner–Hallenda pore size distribution is broadened after the calcination process (Fig. 6). For the exHT silicate sample, the monomodal distribution ranges from 25 to 100 Å, with a peak at 52 Å; furthermore, some of the pores of the precursor are kept in the calcined solid. The exHT carbonate catalyst also shows an enlarged size of the pores after calcination, but in this case a broad and an inhomogeneous pore size distribution is obtained with three maxima at about 34, 44 and 68 Å. In conclusion, the silicate-containing hydrotalcite-like compound leads to catalysts with high specific surface area and a more homogeneous pore size distribution.

4. Conclusions

The physicochemical and textural properties of NiMgAl HTlcs-containing silicates and their decomposition products were studied and compared with those of an HTlc carbonate with the same amount of nickel. PXRD patterns, FT-IR spectroscopy and Thermal Analyses confirm the incorporation of silicates within the interlamellar space. The formation of polysilicate where SiO_4 units condense with the same orientation, thus leading to a reduced crystallinity, is suggested. In addition, mesoporous materials are obtained with a different pore size distribution than in the carbonate sample. After thermal treatment at 900 °C, catalysts show different structures depending on the precursor. Whereas the exHT carbonate shows the MgO- and spinel-type phases, the exHT silicate catalyst shows an additional Mg_2SiO_4 phase and the spinel phase is not well defined. Nevertheless, nickel cations show the same reducibility in both catalysts. However, more studies are in progress in order to obtain more structural information.

Acknowledgements

The financial support from the Italian Ministry of Education (Ministero dell'Istruzione, dell'Università e della Ricerca, PRIN, MIUR, Rome), is gratefully acknowledged.

References

[1] F. Cavani, F. Trifiro, A. Vaccari, Catal. Today 11 (1991) 173.
[2] F. Trifirò, A. Vaccari, in: J.L. Atwood, J.E.D. Davies, D.D. MacNicol, F. Vögtle (Eds.), Comprehensive Supramolecular Chemistry, vol. 7, Pergamon, Oxford, 1996, p. 251.
[3] A. Vaccari, Catal. Today 41 (1998) 53.
[4] B.F. Sels, D.E. De Vos, P.A. Jacobs, Catal. Rev. Sci. Eng. 43 (2001) 443.
[5] F. Basile, A. Vaccari, in: V. Rives (Ed.), Layered Double Hydroxides: Present and Future, Nova Science Publishers, New York, 2001.
[6] A. Monzón, E. Romeo, A.J. Marchi, in: V. Rives (Ed.), Layered Double Hydroxides: Present and Future, Nova Science Publishers, New York, 2001, p. 323.
[7] D. Tichit, B. Coq, Cattech 7 (2003) 206.
[8] S. Albertazzi, F. Basile, A. Vaccari, in: F. Wypych (Ed.), Clay Surfaces: Fundamentals and Applications, Elsevier, Amsterdam, 2004, p. 497.
[9] P. Arpentinier, F. Basile, P. Del Gallo, G. Fornasari, D. Gary, V. Rosetti, A. Vaccari, Catal. Today 99 (2005) 99.
[10] P. Arpentinier, F. Basile, P. del Gallo, G. Fornasari, D. Gary, V. Rosetti, A. Vaccari, Catal. Today 117 (2006) 462.
[11] A. Schultz, P. Biloen, J. Solid State Chem. 68 (1987) 360.
[12] M. del Arco, S. Gutiérrez, C. Martin, V. Rives, J. Rocha, J. Solid State Chem. 151 (2000) 272.
[13] M. del Arco, S. Gutiérrez, C. Martín, V. Rives, Phys. Chem. Chem. Phys. 3 (2001) 119.
[14] C.A. Fyfe, G. Fu, H. Grondey, Mater. Res. Soc. Symp. Proc. 346 (1994) 907.
[15] S.K. Yun, V.R.L. Constantino, T.J. Pinnavaia, Clays Clay Miner. 43 (1995) 503.
[16] C. Misra, J. Perrota, Clays Clay Miner. 40 (1992) 145.
[17] C. Dèpege, F.Z. El Metoui, C. Forano, A. de Roy, J. Dupuis, J.P. Besse, Chem. Mater. 8 (1996) 952.
[18] T. Kloprogge, R.L. Frost, in: V. Rives (Ed.), Layered Double Hydroxides: Present and Future, Nova Sci. Pub. Inc., New York, 2001, p. 155.
[19] E.C. Kruissink, L.L. van Reijden, J.R.H. Ross, J. Chem. Soc. Faraday Trans. I 77 (1981) 649.
[20] V. Rives, in: V. Rives (Ed.), Layered Double Hydroxides: Present and Future, Nova Science Publishers, Inc., New York, 2001, p. 115.
[21] K.S.W. Sing, D.H. Everett, R.A.W. Haul, L. Moscou, R.A. Pierotti, J. Rouquerol, T. Siemieniewska, Pure Appl. Chem. 57 (1985) 603.
[22] F. Rouquerol, J. Rouquerol, K. Sing, Adsorption by Powders and Porous Solids. Principles, Methodology and Applications, Academic Press, London, 1999, p. 441.
[23] G. Fornasari, M. Gazzano, D. Matteuzzi, F. Trifirò, A. Vaccari, Appl. Clay Sci. 10 (1995) 69.
[24] J. Wang, A.M. Davis, R.N. Clayton, A. Hashimoto, Geochem. Cosmochim. Acta 63 (1999) 953.
[25] T.F. Veremeichik, R.V. Galliulin, Inorg. Mater. 38 (2002) 934.
[26] A.B.P. Lever, Inorganic Electronic Spectroscopy, Elsevier, New York, 1984.
[27] W.T. Reichle, Solid State Ionics 22 (1986) 135.